SCIENTIFIC REPORTS

OPEN

Entanglement-Gradient Routing for Quantum Networks

Laszlo Gyongyosi[1,2,3] & Sandor Imre[3]

We define the entanglement-gradient routing scheme for quantum repeater networks. The routing framework fuses the fundamentals of swarm intelligence and quantum Shannon theory. Swarm intelligence provides nature-inspired solutions for problem solving. Motivated by models of social insect behavior, the routing is performed using parallel threads to determine the shortest path via the entanglement gradient coefficient, which describes the feasibility of the entangled links and paths of the network. The routing metrics are derived from the characteristics of entanglement transmission and relevant measures of entanglement distribution in quantum networks. The method allows a moderate complexity decentralized routing in quantum repeater networks. The results can be applied in experimental quantum networking, future quantum Internet, and long-distance quantum communications.

Finding the shortest path in an entangled quantum network is desired for improving the efficiency of quantum repeater networks of the quantum Internet, and of long-distance quantum communications[1–15]. By definition, in an entangled quantum network, the quantum nodes share quantum entanglement. A transmitter and receiver node is separated by several intermediate quantum repeaters, and a chain of entangled links forms a path (entangled path) between the source and destination[16–33]. The level of an entangled link between the quantum nodes determines the achievable hop distance and the number of spanned intermediate nodes. Since quantum networks integrate different levels of entangled links, a shortest path between a source and destination quantum node has to be found in a multi-level quantum network architecture[19–34]. An entangled link has several relevant attributes, such as the level of entanglement (number of nodes spanned by a source-destination path), the entanglement throughput of the link that quantifies the number of entangled states transmitted at a particular fidelity[1–4]. The quantum nodes receive and store the entangled states in their local quantum memories for further extension of the range of entanglement. In the quantum nodes, the number of incoming entangled states represents a crucial parameter from the modeling perspective, along with the mean number of received states (observation rate), and with the reduction in the amount of received entangled states (decay rate).

In this work, we define the *entanglement-gradient routing* scheme for quantum repeater networks. The proposed routing framework fuses the fundamentals of swarm intelligence[35–40] and the results of quantum Shannon theory. Swarm intelligence provides nature-inspired solutions for problem solving. In general, it refers to some population-based meta-heuristics that are motivated by the behavior of living entities (ant colony, bee colony, flock of birds, particle swarm, bacteria foraging, etc.) interacting locally both with each other and the environment. Swarm intelligence has a wide range of applications in real-world problems, ranging from optimization tasks, data mining, computer science, database searching and knowledge discovery to bioinformatics and social networks[35–40].

Our entanglement-gradient routing scheme uses finds the shortest path in a decentralized manner. Motivated by the models of social insect behavior, the routing is relying on several parallel threads, where the threads represent simple, locally interacting individual swarms.

The routing and path selection for quantum repeater networks has been studied in different works[1–5,23–27,41–45]. Without loss of generality, most of these approaches utilized a variance of the well-known Dijsktra's algorithm[45] for the determination of the shortest path in the quantum network. On the other hand, these works have successfully confirmed that a shortest path algorithm from the traditional context is implementable and works well in a quantum environment. In our work we step further, and inject significant novelties to the procedures of

[1]School of Electronics and Computer Science, University of Southampton, Southampton, SO17 1BJ, UK. [2]MTA-BME Information Systems Research Group, Hungarian Academy of Sciences, 7 Nador st., Budapest, H-1051, Hungary. [3]Department of Networked Systems and Services, Budapest University of Technology and Economics, 2 Magyar tudosok krt., Budapest, H-1117, Hungary. Correspondence and requests for materials should be addressed to L.G. (email: l.gyongyosi@soton.ac.uk)

routing and path selection in quantum networks. Our framework breaks with the practice of implementing a Dijsktra-variant algorithm or other, well-known traditional routing protocol in a quantum environment. In our solution, the shortest paths are determined by a biologically-inspired, decentralized algorithm that takes into account the physical-layer attributes of the entanglement establishment and the quantum transmission.

The *entanglement gradient* coefficient quantifies the attractiveness of entangled links and paths for the threads in the quantum repeater network. Each thread acts in a localized manner and the threads are attracted by the entanglement gradients of the paths. The routing is based on metrics that use the tools of quantum Shannon theory. The metrics are derived from the characteristics of entanglement transmission and relevant physical and statistical measures of entanglement distribution. To measure the relevance of a particular entangled link, we define the *entanglement utility* coefficient. Using the entanglement throughput characteristic extractable from the quantum network, we define the *link entanglement gradient* coefficient. We then extend the entanglement gradient for entangled paths (*path entanglement gradient* coefficient), which refers to a path formulated by entangled links.

The aim of using the threads is to find the most attractive path in the quantum network with a highest entanglement gradient (i.e., lowest inverse entanglement gradient) similar to the methods of swarm intelligence. The entanglement gradient evolves in time, decaying as the entanglement throughput deviates from a mean value (decay rate coefficient).

The threads build probabilistic paths between the quantum nodes using simple processing steps to keep minimal the complexity of the scheme. We also include a performance analysis of the routing scheme. The proposed routing method supports a moderate-complexity routing in quantum repeater networks.

Since the proposed framework has no additional physical-layer requirements, the scheme is straightforwardly applicable by current physical devices in an experimental quantum networking scenario. A physical implication of a stationary node in our quantum network model can integrate standard photonics devices[23–27], quantum memories, optical cavities and other fundamental physical devices[1,41,42]. The quantum transmission between the nodes can be realized via noisy quantum links (e.g., optical fibers, wireless quantum channels, free-space optical channels, etc) and fundamental quantum transmission protocols[42].

Since the method is based on the fundamentals of swarm intelligence theory, the proposed framework allows a fusion with the elements of quantum machine learning[43,44]. By utilizing additional functions in the quantum nodes, the model provides a ground for a direct application of a distributed secure quantum machine learning method[48].

The novel contributions of this paper are as follows:

- *We provide a nature-inspired, decentralized routing scheme for quantum repeater networks.*
- *The routing metric utilizes the attributes of entangled links, the properties of entanglement transmission and the statistical distribution of the entangled states in the quantum network.*
- *The method supports an efficient and moderate-complexity routing in quantum repeater networks by fusing the relevant characteristics of entanglement distribution and swarm intelligence theory.*
- *The scheme provides an easy experimental implementation by standard photonics devices, provides a useful tool for shortest path finding in quantum Internet and in practical long-distance quantum communications.*

This paper is organized as follows. In Section 2, the preliminaries and definitions are introduced. Section 3 discusses the entanglement gradient of entangled paths, while Section 4 details the entanglement-gradient routing proposed for quantum repeater networks. In Section 5, a numerical analysis is provided. Finally, Section 6 concludes the paper. Some supplemental information is included in the Appendix.

Preliminaries

In this preliminary section, we summarize the terms and definitions.

Entanglement Utility.

In the proposed model, the relevance of a particular entangled link is characterized by the entanglement utility coefficient, $\lambda_{E_{L_l}(x,y)}$ of an entangled link $E_{L_l}(x, y)$ between nodes x and y, where L_l is the level of the entangled link (By definition, for an L_l-level entangled link, the hop distance between quantum nodes x and y is 2^{l-1}).

This amount is equivalent to the utility of the entangled link $E_{L_l}(x, y)$ that it has taken in order to arrive at the current node y from x (see Fig. 1), and initialized without loss of generality as

$$\lambda_{E_{L_l}(x,y)} \geq 0 \tag{1}$$

Let A be the source quantum node and B the target repeater node. Let y be the current node with a direct neighbor x and an established entangled link $E_{L_l}(x, y)$ between x and y.

Let $B_F\left(E_{L_l}(x, y)\right)$ refer to the *entanglement throughput* of a given L_l-level entangled link $E_{L_l}(x, y)$ between nodes (x, y) measured in the number of d-dimensional entangled states per sec at a particular entanglement fidelity F[1,3,4].

In our scheme, at a given $B_F\left(E_{L_l}(x, y)\right)$, the update of an initial $\lambda_{E_{L_l}(x,y)}$ entanglement utility of link $E_{L_l}(x, y)$ to $\lambda'_{E_{L_l}(x,y)}$[24–26,32,33] is defined as
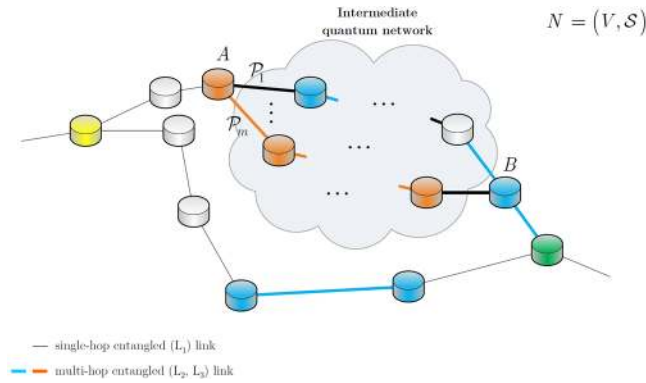
Figure 1. A quantum network with source node A and destination node B, and m entangled paths $\mathcal{P}_1, \ldots, \mathcal{P}_m$ between them. Each path is formulated by a chain of entangled links between quantum repeater nodes. The actual network topology between A and B is unknown (depicted by the cloud) and paths $\mathcal{P}_1, \ldots, \mathcal{P}_m$ abstract all entangled links and noise between A and B. A section of path $\mathcal{P}_1$ is illustrated by an L_l-level entangled link $E_{L_l}(x, y)$ between nodes(x, y) of the particular path.

$$\lambda'_{E_{L_l}(x,y)} = \left(\frac{1}{\lambda_{E_{L_l}(x,y)}} + B_F\left(E_{L_l}(x, y)\right) \right)^{-1}$$
$$= \frac{\lambda_{E_{L_l}(x,y)}}{1 + B_F\left(E_{L_l}(x, y)\right)\lambda_{E_{L_l}(x,y)}}, \tag{2}$$

where $B_F\left(E_{L_l}(x, y)\right)$ serves as a cost function between node pair (x, y) which is added to the inverse of the current entanglement utility, i.e., $1/\lambda_{E_{L_l}(x,y)}$. The update mechanism of (2) is therefore formulates the evolution of entanglement utility in the destination node y. Utilizing the fundamental updating methods of swarm intelligence[38–40,46], (2) provides a solution to take into account not just the characteristic of entanglement transmission, but also the physical attributes of quantum links.

Link Entanglement Gradient. The attractiveness of a particular quantum node is characterized by the link entanglement gradient coefficient. Let $\mathcal{G}^y_{A,x}$ be the amount of entanglement gradient from source node A, on the neighbor node x at y, initialized as $\mathcal{G}^y_{A,x} \geq 0$. The entanglement gradient is updated in a particular quantum node y, as follows.

Motivated by the fundamentals of swarm intelligence theory[38–40,46,47], using (2) the entanglement gradient $\mathcal{G}^y_{A,x}$ (link entanglement gradient) at current node y and entangled link $E_{L_l}(x, y)$ is updated to $\mathcal{G}'^y_{A,x}$ as

$$\mathcal{G}'^y_{A,x} = \mathcal{G}^y_{A,x}f\left(-\tau\left(\Delta B_F\left(E_{L_l}(x, y)\right)\right)\right) + \lambda'_{E_{L_l}(x,y)}, \tag{3}$$

where $\tau \geq 0$ is a decay rate of entanglement gradient, function $f(x)$ provides a probability distribution, while the *entanglement throughput deviation* parameter, $\Delta B_F\left(E_{L_l}(x, y)\right)$, is defined as

$$\Delta B_F\left(E_{L_l}(x, y)\right) = \left| \frac{\sum_{h=1}^{n} B_F\left(E_{L_l}(y, h)\right)}{n} - B_F\left(E_{L_l}(x, y)\right) \right|, \tag{4}$$

where n is the number of direct connections of node y, $\sum_{h=1}^{n} B_F\left(E_{L_l}(y, h)\right)$ is the total entanglement throughput of all n direct links of node y, while $B_F\left(E_{L_l}(x, y)\right)$ is the entanglement throughput of link $E_{L_l}(x, y)$ between nodes y and x.

For all other neighbors j, $j = 1, \ldots, n, j \in V - x$, the entanglement gradient $\mathcal{G}^y_{A,i}$ is only decreased by a factor $f\left(-\tau\left(\Delta B_F\left(E_{L_l}(j, y)\right)\right)\right)$, thus

$$\mathcal{G}'^y_{A,j} = \mathcal{G}^y_{A,j}f\left(-\tau\left(\Delta B_F\left(E_{L_l}(j, y)\right)\right)\right), \tag{5}$$

where

$$\Delta B_F\big(E_{L_l}(j, y)\big) = \left| \frac{\sum_{h=1}^{n} B_F\big(E_{L_l}(y, h)\big)}{n} - B_F\big(E_{L_l}(j, y)\big) \right| \tag{6}$$

where $B_F\big(E_{L_l}(y, i)\big)$ is the entanglement throughput of link $E_{L_l}(y, i)$ between nodes y and i.

By some fundamental theory on swarm intelligence[35–40,46,47], we set the exponential distribution function for $f(x)$, as

$$f(x) = e^x, \tag{7}$$

from which (3) is as

$$\mathcal{G}'^{y}_{A,x} = \mathcal{G}^{y}_{A,x} e^{-\tau\big(\Delta B_F\big(E_{L_l}(x,y)\big)\big)} + \lambda'_{E_{L_l}(x,y)}, \tag{8}$$

while (5) can be rewritten as

$$\mathcal{G}'^{y}_{A,j} = \mathcal{G}^{y}_{A,j} e^{-\tau\big(\Delta B_F\big(E_{L_l}(j,y)\big)\big)} \tag{9}$$

Stochastic Model of Entanglement Utility.

Let focus on the $\mathcal{G}^{y}_{A,x}$ evolution (see (3)) at a given $\lambda_{E_{L_l}(x,y)}$ entanglement utility of link $E_{L_l}(x, y)$ between a current node y, and a previous node x. Since the entanglement utility of a given link $E_{L_l}(x, y)$ evolves in time (see (2)) for $E_{L_l}(x, y)$, the $\lambda_{E_{L_l}(x,y)}$ entanglement utility can be modeled as a non-negative, non-stationary random[38,39] process $X^{y}_{E_{L_l}(x,y)}(t)$, with mean $\mu^{y}_{E_{L_l}(x,y)}(t)$. As follows, $\lambda_{E_{L_l}(x,y)}$ provides a sample of process $X^{y}_{E_{L_l}(x,y)}(t)$.

Let $E\Big[X^{y}_{E_{L_l}(x,y)}(t)\Big]$ be the estimate of $X^{y}_{E_{L_l}(x,y)}(t)$, defined as

$$E[X^{y}_{(E_{(L_l)}(x,y)}(t)] = X^{y}_{(E_{(L_l)}(x,y)}(t) * \Omega_{\mathcal{G}^{y}_{(A,x)}}(t), \tag{10}$$

where $*$ is the convolution operator, while function $\Omega_{\mathcal{G}^{y}_{A,x}}(t)$ is defined as

$$\Omega_{\mathcal{G}^{y}_{A,x}}(t) = e^{-\tau\big(\Delta B_F\big(E_{L_l}(x,y)\big)\big)} U(t), \tag{11}$$

where $U(t)$ is the unit step function.

Assuming that the individual samples of $X^{y}_{E_{L_l}(x,y)}(t)$ within a time period ΔT are determined, a $\perp_{\mathcal{G}^{y}_{A,x}}(\Delta T)$ correlation function can be defined as

$$\perp_{\mathcal{G}^{y}_{A,x}}(\Delta T) = e^{-\tau|\Delta T|}. \tag{12}$$

Link Selection Probability.

Using the entanglement gradient $\mathcal{G}'^{y}_{z,B}$ in a current node y with neighbor node z, the $\mathrm{Pr}^{y}_{E_{L_l}(y,z)}$ probability that from node y the entangled link $E_{L_l}(y, z)$ is selected to reach destination B is defined as

$$\mathrm{Pr}^{y}_{E_{L_l}(y,z)} = \frac{(\mathcal{G}'^{y}_{z,B} + \partial)^{\chi}}{\sum_k (\mathcal{G}'^{y}_{k,B} + \partial)^{\chi}} = \frac{\left(\left(\mathcal{G}^{y}_{z,B} e^{-\tau\big(\Delta B_F\big(E_{L_l}(y,z)\big)\big)} + \lambda'_{E_{L_l}(y,z)}\right) + \partial\right)^{\chi}}{\sum_k \left(\left(\mathcal{G}^{y}_{k,B} e^{-\tau\big(\Delta B_F\big(E_{L_l}(y,k)\big)\big)}\right) + \partial\right)^{\chi}}, \tag{13}$$

where $k \in V - y$, V is the set of nodes of the entangled quantum network N, $\partial \geq 0$ is a threshold parameter, while $X \geq 0$ is a tuning parameter. A source-dependent link selection model is discussed in *Section S.1*.

Path Entanglement-Gradient

The relevance of a particular path of the network is characterized by the path entanglement gradient coefficient.

In this section, we extend the entanglement gradient to entangled paths, which refers to the paths between source and target nodes in the quantum network that are formed by a chain of entangled links between quantum repeaters (i.e., paths of entangled links).

The network model used for the entanglement-gradient routing scheme is illustrated in Fig. 1. There are m entangled paths, $\mathcal{P}_1, \ldots, \mathcal{P}_m$ between a source node A and destination node B. Each entangled path $\mathcal{P}_i$, $i = 1, \ldots, m$, is formulated by a chain of entangled links between quantum repeaters.

Path Metrics.

In this section, we focus on the entanglement gradients of the m entangled paths $\mathcal{P}_1, \ldots, \mathcal{P}_m$ between a source node A and target node B.

Let $\mathcal{G}^{A}_{\mathcal{P}_i}$ refer to the path entanglement gradient of a given entangled path $\mathcal{P}_i$, $i = 1, \ldots, m$ at source node A. Let $\mathcal{G}^{B}_{\mathcal{P}_i}$ be the initial path entanglement gradient of $\mathcal{P}_i$ at destination node B[24–26,32]. Let κ_A be the mean number of

d-dimensional entangled states arriving at A and κ_B be the mean number arriving at B; therefore, the total observation rate is

$$\kappa_{AB} = \kappa_A + \kappa_B. \tag{14}$$

Note that, assuming a symmetrical arrival of the entangled states, $\kappa_A = \kappa_B = \kappa_{AB}/2$.

The derivation of updated $\mathcal{G}'^A_{\mathcal{P}_i}$ at the source node A for a given path $\mathcal{P}_i$ is as follows. Let $\mathcal{G}^A_{\mathcal{P}_i}$ be the initial gradient in A and let $\mathcal{P}_i$, characterized by a $X^A_{\mathcal{P}_i}(t)$, be the non-stationary random process with mean $\mu^A_{\mathcal{P}_i}$ (average value of received entanglement gradient).

First, $\mathcal{G}'^A_{\mathcal{P}_i}$ is decomposed to

$$\mathcal{G}'^A_{\mathcal{P}_i} = \mathcal{G}^{A,(\kappa_A, \tau_A)}_{\mathcal{P}_i} + \mathcal{G}^{A,(\mathcal{P}_i)}_{\mathcal{P}_i} + \mathcal{G}^{A,(\mathcal{P}_j)}_{\mathcal{P}_i}, \tag{15}$$

where the first term, $\mathcal{G}^{A,(\kappa_A, \tau_A)}_{\mathcal{P}_i}$, is the entanglement gradient update in A, evaluated as

$$\mathcal{G}^{A,(\kappa_A, \tau_A)}_{\mathcal{P}_i} = \frac{\kappa_A}{\kappa_{AB}} \left(\frac{\kappa_{AB}}{\kappa_{AB} + \tau_A} \right) \mathcal{G}^A_{\mathcal{P}_i}, \tag{16}$$

where τ_A is the decay rate of A.

The second term $\mathcal{G}^{A,(\mathcal{P}_i)}_{\mathcal{P}_i}$ models the entanglement gradient update for the given path $\mathcal{P}_i$ as

$$\mathcal{G}^{A,(\mathcal{P}_i)}_{\mathcal{P}_i} = \mathrm{Pr}^B_{\mathcal{P}_i} \left(\frac{\kappa_B}{\kappa_{AB}} \left(\left(\frac{\kappa_{AB}}{\kappa_{AB} + \tau_A} \right) \mathcal{G}^A_{\mathcal{P}_i} + \left(\mu^A_{\mathcal{P}_i} \right) \right) \right), \tag{17}$$

where $\mu^A_{\mathcal{P}_i}$ is the average value of received entanglement gradient from path $\mathcal{P}_i$ at node A, while $\mathrm{Pr}^B_{\mathcal{P}_i}$ is the probability that path $\mathcal{P}_i$ will be used by B, $\mathrm{Pr}^B_{\mathcal{P}_i} = \left(\mathcal{G}^B_{\mathcal{P}_i} + \partial \right)^\chi / \sum_m \left(\mathcal{G}^B_{\mathcal{P}_i} + \partial \right)^\chi$.

The third term, $\mathcal{G}^{A,(\mathcal{P}_j)}_{\mathcal{P}_i}$ models the path entanglement gradient update for a different path $\mathcal{P}_j, j \neq i$ as

$$\mathcal{G}^{A,(\mathcal{P}_j)}_{\mathcal{P}_i} = \mathrm{Pr}^B_{\mathcal{P}_j} \left(\frac{\kappa_B}{\kappa_{AB}} \left(\left(\frac{\kappa_{AB}}{\kappa_{AB} + \tau_A} \right) \mathcal{G}^A_{\mathcal{P}_i} \right) \right), \tag{18}$$

where $\mathrm{Pr}^B_{\mathcal{P}_j}$ is the probability that $\mathcal{P}_j$ will be used by B, $\mathrm{Pr}^B_{\mathcal{P}_j} = \left(\mathcal{G}^B_{\mathcal{P}_j} + \partial \right)^\chi / \sum_m \left(\mathcal{G}^B_{\mathcal{P}_i} + \partial \right)^\chi$.

From (16), (17), and (18), $\mathcal{G}'^A_{\mathcal{P}_i}$ in (15) can be rewritten for a particular path $\mathcal{P}_i$ as

$$\mathcal{G}'^A_{\mathcal{P}_i} = \left(\frac{\kappa_{AB}}{\kappa_{AB} + \tau_A} \right) \mathcal{G}^A_{\mathcal{P}_i} + \left(\frac{\kappa_B}{\kappa_{AB}} \right) \mathrm{Pr}^B_{\mathcal{P}_i} \left(\mu^A_{\mathcal{P}_i} \right). \tag{19}$$

Following the same steps for path $\mathcal{P}_j, j \neq i, \mathcal{G}'^A_{\mathcal{P}_j}$ is evaluated at node A, for all instances of j, as

$$\mathcal{G}'^A_{\mathcal{P}_j} = \left(\frac{\kappa_{AB}}{\kappa_{AB} + \tau_A} \right) \mathcal{G}^A_{\mathcal{P}_j} + \left(\frac{\kappa_B}{\kappa_{AB}} \right) \mathrm{Pr}^B_{\mathcal{P}_j} \left(\mu^A_{\mathcal{P}_j} \right). \tag{20}$$

At target node B, the corresponding formula for path $\mathcal{P}_i, \mathcal{G}'^B_{\mathcal{P}_i}$ is therefore yielded as

$$\mathcal{G}'^B_{\mathcal{P}_i} = \left(\frac{\kappa_{AB}}{\kappa_{AB} + \tau_B} \right) \mathcal{G}^B_{\mathcal{P}_i} + \left(\frac{\kappa_A}{\kappa_{AB}} \right) \mathrm{Pr}^A_{\mathcal{P}_i} \left(\mu^B_{\mathcal{P}_i} \right), \tag{21}$$

where $\mu^B_{\mathcal{P}_i}$ is the average value of received entanglement gradient from path $\mathcal{P}_i$ at node B, $\mathrm{Pr}^A_{\mathcal{P}_i}$ is the probability that path $\mathcal{P}_i$ will be used by A, and $\mathrm{Pr}^A_{\mathcal{P}_i} = \left(\mathcal{G}^A_{\mathcal{P}_i} + \partial \right)^\chi / \sum_m \left(\mathcal{G}^A_{\mathcal{P}_i} + \partial \right)^\chi$.

The formula of $\mathcal{G}'^B_{\mathcal{P}_j}$ for path $\mathcal{P}_j, j \neq i$ at target node B is therefore

$$\mathcal{G}'^B_{\mathcal{P}_j} = \left(\frac{\kappa_{AB}}{\kappa_{AB} + \tau_B} \right) \mathcal{G}^B_{\mathcal{P}_j} + \left(\frac{\kappa_A}{\kappa_{AB}} \right) \mathrm{Pr}^A_{\mathcal{P}_j} \left(\mu^B_{\mathcal{P}_j} \right), \tag{22}$$

where $\mathrm{Pr}^A_{(P_j)}$ is $\mathrm{Pr}^A_{(P_j)} = (\mathcal{G}^A_{(P_j)} + \partial)^\chi / \sum_m (\mathcal{G}^A_{(P_i)} + \partial)^\chi$.

For the $\mathcal{P}^*$ optimal shortest path, the entanglement gradient is maximal, thus $\mathcal{G}'^A_{\mathcal{P}^*}$ is determined as

$$\mathcal{G}'^A_{\mathcal{P}^*} = \max_{\forall i} \mathcal{G}'^A_{\mathcal{P}_i}$$
$$= \left(\frac{\kappa_{AB}}{\kappa_{AB} + \tau_A} \right) \mathcal{G}^A_{\mathcal{P}^*} + \left(\frac{\kappa_B}{\kappa_{AB}} \right) \mathrm{Pr}^B_{\mathcal{P}^*} \left(\mu^A_{\mathcal{P}^*} \right), \tag{23}$$

Mean of path entanglement gradient. After some calculations, the mean entanglement gradient $\mathbb{E}\left(\mathcal{G}'^{A}_{\mathcal{P}_i}\right)$ of a particular path $\mathcal{P}_i$ at A is obtainable if the path $\mathcal{P}_i$ is selected with unit probability in A, $\mathrm{Pr}^{A}_{\mathcal{P}_i} = 1$, yielding $\mathbb{E}\left(\mathcal{G}'^{A}_{\mathcal{P}_i}\right)$ as

$$\mathbb{E}(\mathcal{G}'^{A}_{\mathcal{P}_i}) = \frac{(\kappa_{AB} + \tau_A)\kappa_B}{\kappa_{AB}\tau_A}\mu^{A}_{\mathcal{P}_i}. \tag{24}$$

By similar assumptions, the $\mathbb{E}\left(\mathcal{G}'^{B}_{\mathcal{P}_i}\right)$ mean entanglement gradient of a particular path $\mathcal{P}_i$ at B, obtainable at $\mathrm{Pr}^{B}_{\mathcal{P}_i}=1$, is

$$\mathbb{E}\left(\mathcal{G}'^{B}_{\mathcal{P}_i}\right) = \frac{(\kappa_{AB} + \tau_B)\kappa_A}{\kappa_{AB}\tau_B}\mu^{B}_{\mathcal{P}_i}. \tag{25}$$

Decay Rate of Mean Path Entanglement Gradient. A crucial parameter for the optimization of the entanglement-gradient routing is the $\tau_{\mathcal{G}'^{n}_{\mathcal{P}_i}}$ decay rate of mean path entanglement gradient $\mathbb{E}\left(\mathcal{G}'^{n}_{\mathcal{P}_i}\right)$.

Without loss of generality, at a given expected amount of entanglement gradient $\mathbb{E}\left(\mathcal{G}'^{n}_{\mathcal{P}_i}\right)$ at node n for path $\mathcal{P}_i$, the threshold $\partial_{\mathbb{E}\left(\mathcal{G}'^{n}_{\mathcal{P}_i}\right)}$ can be rewritten as:

$$\partial_{\mathbb{E}\left(\mathcal{G}'^{n}_{\mathcal{P}_i}\right)} = \mathbb{E}\left(\mathcal{G}'^{n}_{\mathcal{P}_i}\right)e^{-\varphi(\mathcal{P}_i)\tau_{\mathbb{E}\left(\mathcal{G}'^{n}_{\mathcal{P}_i}\right)}}, \tag{26}$$

where $\varphi(\mathcal{P}_i)$ characterizes the deviation of a current $B_F(\mathcal{P}_i)$ entanglement throughput (measured in d-dimensional entangled states of a particular fidelity F per sec) of path $\mathcal{P}_i$ from an expected $\widetilde{B}_F(\mathcal{P}_i)$ entanglement throughput of path $\mathcal{P}_i$ as

$$\varphi(\mathcal{P}_i) = \left|\widetilde{B}_F(\mathcal{P}_i) - B_F(\mathcal{P}_i)\right|. \tag{27}$$

and therefore $\tau_{\mathbb{E}\left(\mathcal{G}'^{n}_{\mathcal{P}_i}\right)}$ is[38–40,46]

$$\tau_{\mathbb{E}\left(\mathcal{G}'^{n}_{\mathcal{P}_i}\right)} = -\ln\frac{\partial_{\mathbb{E}\left(\mathcal{G}'^{n}_{\mathcal{P}_i}\right)}}{\mathbb{E}\left(\mathcal{G}'^{n}_{\mathcal{P}_i}\right)\varphi(\mathcal{P}_i)} = -\ln\frac{\partial_{\mathbb{E}\left(\mathcal{G}'^{n}_{\mathcal{P}_i}\right)}}{\mathbb{E}\left(\mathcal{G}'^{n}_{\mathcal{P}_i}\right)\left|\widetilde{B}_F(\mathcal{P}_i) - B_F(\mathcal{P}_i)\right|}. \tag{28}$$

Optimal estimator. The $\widetilde{\tau}_{\mathbb{E}\left(\mathcal{G}'^{n}_{\mathcal{P}_i}\right)}$ optimal estimator of $\tau_{\mathbb{E}\left(\mathcal{G}'^{n}_{\mathcal{P}_i}\right)}$ is derived as follows. Using (12) with (27) allows us to evaluate a variable Y as

$$Y = \perp_{\mathbb{E}\left(\mathcal{G}'^{n}_{\mathcal{P}_i}\right)}(\varphi(\mathcal{P}_i)) = e^{-\widetilde{\tau}_{\mathbb{E}\left(\mathcal{G}'^{n}_{\mathcal{P}_i}\right)}\varphi(\mathcal{P}_i)}, \tag{29}$$

from which the $\widetilde{\tau}_{\mathbb{E}\left(\mathcal{G}'^{n}_{\mathcal{P}_i}\right)}$ optimal estimate of the $\tau_{\mathbb{E}\left(\mathcal{G}'^{n}_{\mathcal{P}_i}\right)}$ of $\mathbb{E}\left(\mathcal{G}'^{n}_{\mathcal{P}_i}\right)$ is yielded as[38–40,46]

$$\widetilde{\tau}_{\mathbb{E}\left(\mathcal{G}'^{n}_{\mathcal{P}_i}\right)} = -\frac{\ln Y}{\varphi(\mathcal{P}_i)} = -\frac{\ln\left(e^{-\widetilde{\tau}_{\mathbb{E}\left(\mathcal{G}'^{n}_{\mathcal{P}_i}\right)}\varphi(\mathcal{P}_i)}\right)}{\varphi(\mathcal{P}_i)}. \tag{30}$$

At a given optimal decay rate $\widetilde{\tau}_{\mathbb{E}\left(\mathcal{G}'^{n}_{\mathcal{P}_i}\right)}$ (30), using (24) in (26) results in $\partial_{\mathbb{E}\left(\mathcal{G}'^{n}_{\mathcal{P}_i}\right)}$ as

$$\partial_{\mathbb{E}\left(\mathcal{G}'^{n}_{\mathcal{P}_i}\right)} = \frac{\left(\kappa_{AB} + \widetilde{\tau}_{\mathbb{E}\left(\mathcal{G}'^{n}_{\mathcal{P}_i}\right)}\right)}{2\widetilde{\tau}_{\mathbb{E}\left(\mathcal{G}'^{n}_{\mathcal{P}_i}\right)}}\mu^{n}_{\mathcal{P}_i}e^{-\widetilde{\tau}_{\mathbb{E}\left(\mathcal{G}'^{n}_{\mathcal{P}_i}\right)}\varphi(\mathcal{P}_i)}. \tag{31}$$

Path Selection. A brief description of the method to determine the entanglement gradient of the paths for characterization of an optimal path $\mathcal{P}^*$ is as follows.

Method

Step 1. Let $n-1$ and n be a pair of neighbor quantum repeaters of a path between source node A and target node B. Let n be the current node, $n-1$ be the previous node, and $n+1$ be a next node.

Step 2. Apply (2) to increase the entanglement utility of the entangled link between $n-1$ and n. For node $n-1$, increase entanglement gradient via (3). For all other neighboring nodes, decrease entanglement gradient via (5).

Step 3. From the updated entanglement gradients, compute $\mathrm{Pr}^{n}_{E_{L_i}(n,n+1)}$ of entangled link $E_{L_i}(n, n+1)$ via (13).

Step 4. Apply steps 1–3 for all nodes and paths, $\mathcal{P}_1, \ldots, \mathcal{P}_m$. Determine optimal $\widetilde{\tau}$ via (30) to set τ.

Step 5. Using (23), output optimal path $\mathcal{P}^*$ for which the entanglement gradient is maximal is $\mathcal{G}'^{A}_{\mathcal{P}^*} = \max_{\forall i}\mathcal{G}'^{A}_{\mathcal{P}_i}$.
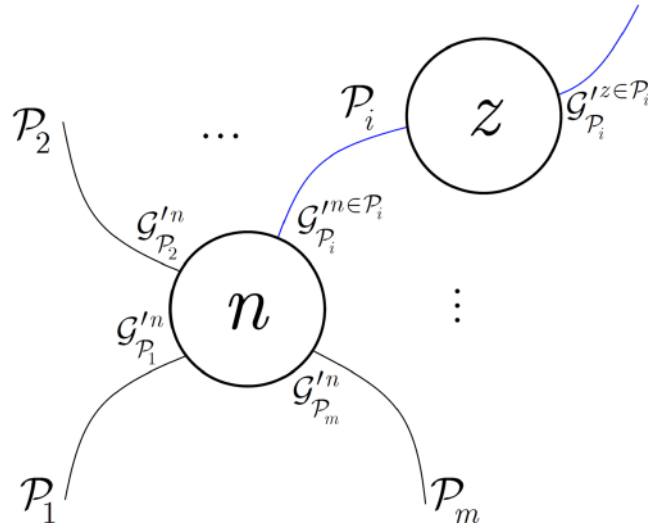
Figure 2. A model of m paths $\mathcal{P}_1$, …, $\mathcal{P}_m$ between a source node s and a current node n. The paths have entanglement gradients $\mathcal{G}'^n_{\mathcal{P}_i}$, $i = 1$, …, m. Current node n and next node z are elements of a current path $\mathcal{P}_i$ (blue), with $\mathcal{G}'^{n\in\mathcal{P}_i}_{\mathcal{P}_i}$ in n and $\mathcal{G}'^{z\in\mathcal{P}_i}_{\mathcal{P}_i}$ in z.

Entanglement-Gradient Routing

In this section, we define a decentralized routing scheme that merges the results of the previous sections on the quantities of entanglement gradient. The routing is executed through parallel threads that simultaneously explore the quantum network. A given thread operates in a localized manner.

Link Selection. For a given path $\mathcal{P}_i$ between a source node s and current node n, a quantity $\Phi^{s,n}_{\mathcal{P}_i}$ is defined as

$$\Phi^{s,n}_{\mathcal{P}_i} = \sum_{x=s}^{n} \alpha \sigma^x_{\mathcal{P}_i},$$

(32)

where

$$\sigma^x_{\mathcal{P}_i} = \log\left(\frac{\mathcal{G}'^{x+1\in\mathcal{P}_i}_{\mathcal{P}_i}}{\mathcal{G}'^{x\in\mathcal{P}_i}_{\mathcal{P}_i}}\right),$$

(33)

where $\mathcal{G}'^{x\in\mathcal{P}_i}_{\mathcal{P}_k}$ is the entanglement gradient of node $x \in \mathcal{P}_i$, $\mathcal{G}'^{x+1\in\mathcal{P}_i}_{\mathcal{P}_k}$ is the entanglement gradient at node $x+1\in\mathcal{P}_i$, and α is

$$\alpha = \begin{cases} 1, & if \left|\sigma^x_{\mathcal{P}_i}\right| > \vartheta \\ 0, & if \left|\sigma^x_{\mathcal{P}_i}\right| \leq \vartheta \end{cases},$$

(34)

where ϑ is a threshold[40].

Using (32), a mean $\mu^n(\Phi^{s,n}_{\mathcal{P}})$ for the m paths $\mathcal{P}_1$, …, $\mathcal{P}_m$ between a source node s and a current node n is

$$\mu^n(\Phi^{s,n}_{\mathcal{P}}) = \frac{\sum_{i=1}^{m} \Phi^{s,n}_{\mathcal{P}_i}}{m}.$$

(35)

A model of a node n with next node z and m paths $\mathcal{P}_1$, …, $\mathcal{P}_m$ between a source node s is depicted in Fig. 2. The entanglement gradients are $\mathcal{G}'^n_{\mathcal{P}_i}$, $i = 1$, …, m. Nodes n and z are elements of a current path $\mathcal{P}_i$, with corresponding entanglement gradients $\mathcal{G}'^{n\in\mathcal{P}_i}_{\mathcal{P}_i}$ and $\mathcal{G}'^{z\in\mathcal{P}_i}_{\mathcal{P}_i}$. From the path gradients, the quantities of $\sigma^x_{\mathcal{P}_i}$ (33) and α (34) are derived to evaluate $\Phi^{s,n}_{\mathcal{P}_i}$ in (32).

Let z be the next node from actual node n on a current path $\mathcal{P}_i$ with entangled connection $E_{L_l}(n, z)$. Then, for $E_{L_l}(n, z)$, the distance function $\psi(n, z)$ between n and z is defined as

$$\psi(n, z) = \left(\frac{1}{\Pr^n_{E_{L_l}(n,z)}}\right)\left|\mathbb{E}\left(\mathcal{G}'^n_{\mathcal{P}_i}\right) - \mathbb{E}\left(\mathcal{G}'^z_{\mathcal{P}_i}\right)\right|$$

$$= \left(\frac{\sum_k (\mathcal{G}'^n_{k,B} + \partial)^\chi}{(\mathcal{G}'^n_{z,B} + \partial)^\chi}\right)\left|\mathbb{E}\left(\mathcal{G}'^n_{\mathcal{P}_i}\right) - \mathbb{E}\left(\mathcal{G}'^z_{\mathcal{P}_i}\right)\right|,$$

(36)

where $\Pr^n_{E_{L_l}(n,z)}$ is (13), while $\mathbb{E}\left(\mathcal{G}'^n_{\mathcal{P}_i}\right)$ and $\mathbb{E}\left(\mathcal{G}'^z_{\mathcal{P}_i}\right)$ are the mean entanglement gradients at nodes $n \in \mathcal{P}_i$ and $z \in \mathcal{P}_i$, evaluated via (24) and (25) as

$$\mathbb{E}\left(\mathcal{G}'^n_{\mathcal{P}_i}\right) = \frac{(\kappa_{nz} + \tau_n)\kappa_z}{\kappa_{nz}\tau_n}\mu^n_{\mathcal{P}_i}, \tag{37}$$

where $\mu^n_{\mathcal{P}_i}$ is the average value of the received entanglement gradient from path $\mathcal{P}_i$ at node n, and

$$\mathbb{E}\left(\mathcal{G}'^z_{\mathcal{P}_i}\right) = \frac{(\kappa_{nz} + \tau_z)\kappa_n}{\kappa_{nz}\tau_z}\mu^z_{\mathcal{P}_i}, \tag{38}$$

where $\mu^z_{\mathcal{P}_i}$ is the average value of the received entanglement gradient from path $\mathcal{P}_i$ at node z, respectively.

The decentralized routing is accomplished via t parallel threads, $\mathcal{T}_1, \ldots, \mathcal{T}_t$. For all threads, a threshold $\ell_{\mathcal{T}}$ is defined, which determines the maximal number of nodes to be explored. Using the $\mathcal{G}'^z_{A,n}$ entanglement link gradient (see (8)), with the entanglement utility $\lambda'_{E_{L_l}(n,z)}$ (2) of link $E_{L_l}(n, z)$ between nodes n and z, an inverse link entanglement gradient $\theta^z_{E_{L_l}(n,z)}$ is defined as

$$\theta^z_{E_{L_l}(n,z)} = \frac{1}{\mathcal{G}'^z_{A,n}} = \frac{1}{\mathcal{G}^z_{A,n}e^{-\tau\left(\Delta B_F\left(E_{L_l}(n,z)\right)\right)} + \lambda'_{E_{L_l}(n,z)}}, \tag{39}$$

where $\lambda'_{E_{L_l}(n,z)}$ is

$$\lambda'_{E_{L_l}(n,z)} = \frac{\lambda_{E_{L_l}(n,z)}}{1 + B_F\left(E_{L_l}(n, z)\right)\lambda_{E_{L_l}(n,z)}}. \tag{40}$$

Then, for a given i-th thread $\mathcal{T}_i$, the $p_{\mathcal{T}_i}(n, z)$ link selection probability is defined as

$$p_{\mathcal{T}_i}(n, z) = \begin{cases} \Pr_{\mathcal{T}_i}(n, z), & \text{if } z \notin S_{\mathcal{T}_i} \\ 0, & \text{otherwise}, \end{cases} \tag{41}$$

where $S_{\mathcal{T}_i}$ is a set of nodes already visited by the i-th thread $\mathcal{T}_i$[40], while $\Pr_{\mathcal{T}_i}(n, z)$ is

$$\Pr_{\mathcal{T}_i}(n, z) = \frac{\left(\theta^z_{E_{L_l}(n,z)}\right)^{C_1}(\psi(n, z))^{C_2}}{\sum_{k \notin S_{\mathcal{T}_i}}\left(\theta^k_{E_{L_l}(n,k)}\right)^{C_1}(\psi(n, k))^{C_2}}, \tag{42}$$

where $k \notin S_{\mathcal{T}_i}, C_1$, and C_2 are weighting parameters to balance the relevance between inverse entanglement gradient function $\theta(\,\cdot\,)$ and distance function $\psi(\,\cdot\,)$.

The remaining quantities of (42) are evaluated as

$$\theta^k_{E_{L_l}(n,k)} = \frac{1}{\mathcal{G}'^k_{A,n}}, \tag{43}$$

and

$$\psi(n, k) = \Pr^n_{E_{L_l}(n,k)}\left|\mathbb{E}\left(\mathcal{G}'^n_{\mathcal{P}_i}\right) - \mathbb{E}\left(\mathcal{G}'^k_{\mathcal{P}_i}\right)\right|. \tag{44}$$

Algorithm. A brief description of the entanglement-gradient routing algorithm $\mathcal{A}_{\mathcal{G}}$ for finding the shortest path via the entanglement gradient is as follows.

Algorithm (entanglement-gradient routing).

Step 1. Set t and $\ell_{\mathcal{T}}$ for threads $\mathcal{T}_1, \ldots, \mathcal{T}_t$, where $\ell_{\mathcal{T}}$ is a thread-threshold that limits the maximal number of nodes to be explored to $\ell_{\mathcal{T}}$ by a given $\mathcal{T}_i$. For a given $\mathcal{T}_i$, let $S_{\mathcal{T}_i}$ be a set of already visited nodes.

Step 2. For a thread $\mathcal{T}_i$, given node n and next node z, determine $p_{\mathcal{T}_i}(n, z)$ via (41). If $z \notin S_{\mathcal{T}_i}$, set $p_{\mathcal{T}_i}(n, z) = 0$; otherwise, calculate $\Pr_{\mathcal{T}_i}(n, z)$ via (42).

Step 3. As a next node $n + 1$ is determined, update inverse link entanglement gradient $\theta^{n+1}_{E_{L_l}(n,n+1)}$ via (39).

Step 4. Apply steps 1–3 for all threads, $\mathcal{T}_1, \ldots, \mathcal{T}_t$.

Discussion

In $\mathcal{A}_{\mathcal{G}}$, any thread $\mathcal{T}_i$ at a given step selects that node for which the entanglement gradient is high, i.e., the inverse link entanglement gradient of the entangled connection is low. When the inverse link entanglement gradient is high, the threads choose a different direction and entangled links. The thread threshold $\ell_{\mathcal{T}}$ allows for focus on a particular subset of the network for an optimal parallel realization. The distance function of (36) takes into consideration not just the absolute entanglement-gradient difference but also the inverse of the probability of the
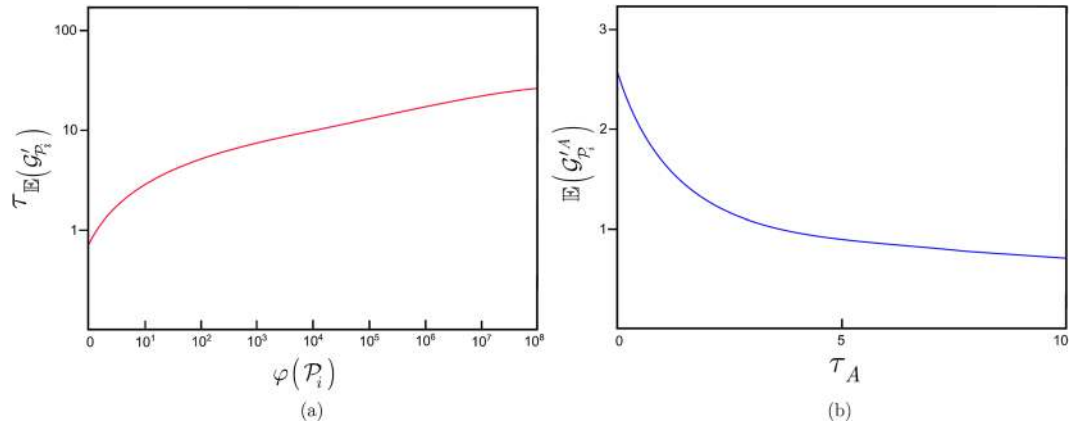
Figure 3. (a) The decay rate $\tau_{\mathbb{E}(\mathcal{G}'_{\mathcal{P}_i})}$ (log-scale) of entanglement gradient $\mathbb{E}(\mathcal{G}'_{\mathcal{P}_i})$ for path $\mathcal{P}_i$, $\varphi(\mathcal{P}_i) = 10^0, \ldots, 10^8$, and $\partial = 1$, $\mathbb{E}(\mathcal{G}'_{\mathcal{P}_i}) = 2$. (b) The $\mathbb{E}(\mathcal{G}'^A_{\mathcal{P}_i})$ of a path $\mathcal{P}_i$ at node A as a function of τ_A at $\kappa_{AB} = 4$, $\kappa_B = 2$ and $\mu^A_{\mathcal{P}_i} = 1$.

selection of a given entangled link. The threads also change their behavior as the entanglement-gradients evolve in the network, which yields dynamically changing adaptive searching.

For a given thread $\mathcal{T}_i$, the C_1 and C_2 weighting coefficients are crucial in the probability function of (42) for determining the local behavior of a given thread (e.g., the routing is decentralized). The selection method of these weights is discussed next.

Computational Complexity. The computational complexity of the entanglement-gradient routing at $|N|$ nodes, with t parallel threads and a thread-threshold $\ell_{\mathcal{T}}$, is at most

$$\mathcal{O}(|N| t \ \ell_{\mathcal{T}}). \tag{45}$$

The result of (45) can be verified easily, since the maximal number of nodes visited by a given thread $\mathcal{T}_i$ is at most $\ell_{\mathcal{T}}$.

Numerical Evidence

In this section, we analyze the performance metrics of the link and path selection phases and the entanglement-gradient routing.

Link and Path Metrics. In this section, the proposed link and path metrics are analyzed. The decay rate $\tau_{\mathbb{E}(\mathcal{G}'_{\mathcal{P}_i})}$ (28) of entanglement gradient $\mathbb{E}(\mathcal{G}'_{\mathcal{P}_i})$ for various $\varphi(\mathcal{P}_i)$ at $\partial_{\mathbb{E}(\mathcal{G}'_{\mathcal{P}_i})} = 1$ and $\mathbb{E}(\mathcal{G}'_{\mathcal{P}_i}) = 2$ is depicted in Fig. 3(a). The $\tau_{\mathbb{E}(\mathcal{G}'_{\mathcal{P}_i})}$ decay rate of entanglement gradient increases with the $\varphi(\mathcal{P}_i)$ parameter of the given path $\mathcal{P}_i$. As the $B_F(\mathcal{P}_i)$ entanglement throughput of that path $\mathcal{P}_i$ significantly deviates from the expected average $\widetilde{B}_F(\mathcal{P}_i)$, the entanglement gradient of $\mathcal{P}_i$ decreases more significantly.

In Fig. 3(b), the $\mathbb{E}(\mathcal{G}'^A_{\mathcal{P}_i})$ (see (24)) of a particular path $\mathcal{P}_i$ at node A, as a function of τ_A at $\kappa_{AB} = 4$, $\kappa_B = 2$ and $\mu^A_{\mathcal{P}_i} = 1$, is depicted.

Without loss of generality, at a given κ_n in a node n, let ν_n be defined as

$$\frac{-2\pi}{\kappa_n} \le \nu_n \le \frac{2\pi}{\kappa_n}. \tag{46}$$

Then, rewrite $\mathbb{E}(\mathcal{G}'^n_{\mathcal{P}_i}(\nu_n))$ as

$$\mathbb{E}(\mathcal{G}'^n_{\mathcal{P}_i}(\nu_n)) = \mu^n_{\mathcal{P}_i} \varsigma(\gamma_n), \tag{47}$$
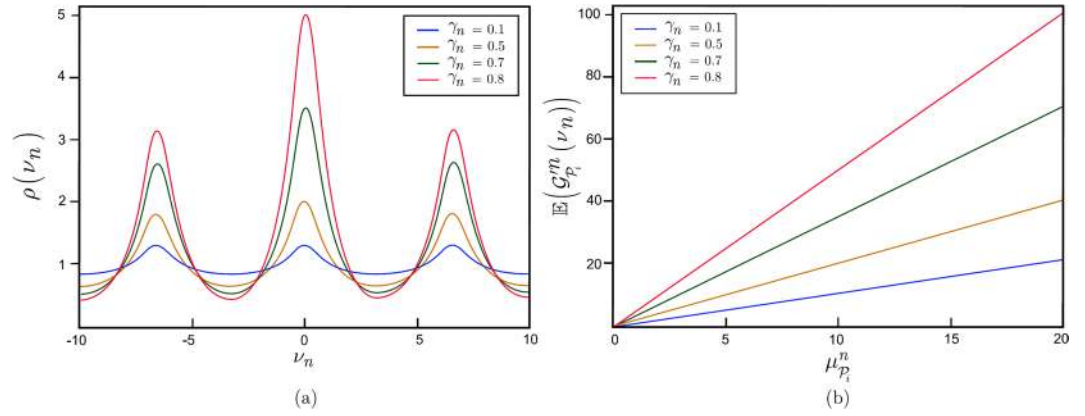
where $\varsigma(\gamma_n)$ is a peak of function $\rho(\nu_n)$ and $\rho(\nu_n)$ is

$$\rho(\nu_n) = \frac{1}{\sqrt{1 + \gamma_n^2 - 2\gamma_n \cos(\nu_n)}}, \tag{48}$$

where γ_n is

$$\gamma_n = \frac{\kappa_n}{\kappa_n + \tau_n} = \left(1 + \frac{\tau}{\kappa_n}\right)^{-1}, \tag{49}$$

where κ_n is the observation rate in node n and τ_n is the decay rate of the entanglement gradient in node n.

Figure 4. (a) The values of $\rho(\nu_n)$ as a function of ν_n for $\gamma_n = 0.1$, 0.5, 0.8, 0.9 at node n. The $\varsigma(\gamma_n)$ peak of $\rho(\nu_n)$ at a given γ_n is $\varsigma(\gamma_n) = 1/(1 - \gamma_n)$. **(b)** The mean $\mathbb{E}\left(\mathcal{G}'^n_{\mathcal{P}_i}(\nu_n)\right) = \mu^n_{\mathcal{P}_i}\varsigma(\gamma_n)$ entanglement gradient received from path $\mathcal{P}_i$ as a function of $\mu^n_{\mathcal{P}_i}$ for a $\gamma_n = 0.1$, 0.5, 0.8, 0.9.

The quantity of $\varsigma(\gamma_n)$ is derived as follows. The formula of $\rho(\nu_n)$ (see (48)) can be rewritten as a magnitude

$$\rho(\nu_n) = |\mathcal{F}(\nu_n)|. \tag{50}$$

where $\mathcal{F}(\nu_n)$ is defined as

$$\mathcal{F}(\nu_n) = \frac{1}{1 - \gamma_n e^{-i\nu_n}}. \tag{51}$$

Thus, the peak $\varsigma(\gamma_n)$ of $\rho(\nu_n)$ at a given γ_n is yielded as

$$\varsigma(\gamma_n) = \frac{1}{(1 - \gamma_n)}. \tag{52}$$

At a given γ_n and mean $\mu^n_{\mathcal{P}_i}$ (average value of received entanglement gradient) at node n for path $\mathcal{P}_i$, the mean of the received entanglement gradient can be rewritten from $\varsigma(\gamma_n)$ (see (52)) as

$$\mathbb{E}\left(\mathcal{G}'^n_{\mathcal{P}_i}(\nu_n)\right) = \mu^n_{\mathcal{P}_i}\varsigma(\gamma_n) = \frac{\mu^n_{\mathcal{P}_i}}{(1 - \gamma_n)}. \tag{53}$$

The value of $\rho(\nu_n)$ as a function of ν_n for various γ_n is depicted in Fig. 4(a). The resulting mean entanglement gradient $\mathbb{E}\left(\mathcal{G}'^n_{\mathcal{P}_i}(\nu_n)\right)$, as a function of $\mu^n_{\mathcal{P}_i}$ for various γ_n of path $\mathcal{P}_i$ at node n, is depicted in Fig. 4(b). As the $\mu^n_{\mathcal{P}_i}$ average value of the received entanglement gradient increases, the mean entanglement gradient $\mathbb{E}\left(\mathcal{G}'^n_{\mathcal{P}_i}(\nu_n)\right)$ becomes more significant, specifically for high values of γ_n.

At a $0 \leq \Pi \leq 1$ tuning parameter (a fraction of peak value), let κ_n^* be a cutoff observation rate (critical received d-dimensional entangled states per sec) defined at a given observation rate κ_n as

$$\kappa_n^* = \frac{\kappa_n}{2\pi}\cos^{-1}\left(\frac{\kappa_n^2 + \kappa_n\tau_n - \frac{\tau_n^2 + \Pi^2\tau_n^2}{2\Pi^2}}{\kappa_n^2 + \kappa_n\tau_n}\right). \tag{54}$$

If $\kappa_n > \kappa_n^*$ at a given τ_n and Π, then in node n, the value of the total received entanglement gradient will not adapt to the actually received total value of entanglement gradients, i.e., κ_n^* serves a cutoff in the observation rate.

The values of κ_n^* as a function of τ_n for various κ_n at $\Pi = 0.5$ (in analogue to a -3 dB cutoff[38–40,46]) are shown in Fig. 5. The κ_n^* cutoff observation rate is controllable by τ_n and the impact of an actual κ_n rate on κ_n^* is almost negligible.

Decentralized Routing. The routing procedure is discussed by the $\Pr_{\mathcal{T}_i}(n, z)$ probability function of (42). In (42), the C_1 and C_2 weights have a crucial role and are determined as follows.

If the average value $\mu^n(\Phi^{s,n}_{\mathcal{P}})$ (see (35)) is low, then C_1 is high and C_2 is low. In this case an another way and a different node but not z is selected at an actual node n. For a high $\mu^n(\Phi^{s,n}_{\mathcal{P}})$, C_2 picks up a high value and C_1 is low. In this case the current target node z is selected at node n.

Thus, for a given threshold o on $\mu^n(\Phi^{s,n}_{\mathcal{P}})$, $\mu^n(\Phi^{s,n}_{\mathcal{P}}) \leq o$, the selection rule for weights $\{C_1, C_2\}$ is
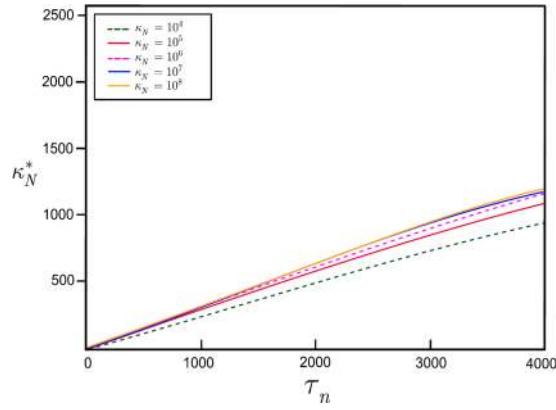
Figure 5. The values of κ_n^* as a function of τ_n for $\kappa_n = 10^4, 10^5, 10^6, 10^7, 10^8$ at $\Pi = 0.5$.
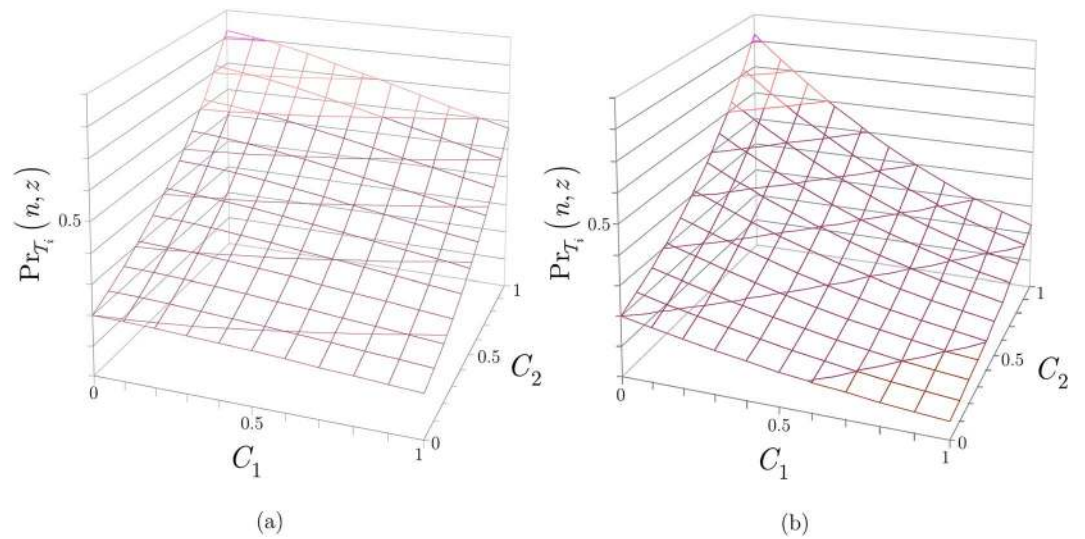
Figure 6. (a) The $\mathrm{Pr}_{\mathcal{T}_i}(n, z)$ probability of selecting a next node z from a current node n for a given path $\mathcal{P}_i$, $0 \leq C_1 \leq 1$ and $0 \leq C_2 \leq 1$, at a setting of $\theta_{E_{L_l}(n,z)}^z = 0.5, \psi(n, z) = 5, k = 5$, and at (b) $\theta_{E_{L_l}(n,z)}^z = 0.2$, $\psi(n, z) = 5, k = 5$.

$$\{C_1, C_2\} = \begin{cases} C_1 \to 1, C_2 \to 0, \; if \mu^n(\Phi_{\mathcal{P}}^{s,n}) \leq o, \\ C_1 \to 0, C_2 \to 1, \; otherwise. \end{cases} \tag{55}$$

As a corollary of (55), a high value of C_1 and a low value of C_2 increases the network area to be explored by a thread, while for a low value of C_1 and a high value of C_2, the number of explored nodes is smaller.

The values of $\mathrm{Pr}_{\mathcal{T}_i}(n, z)$ (42) as a function of weight coefficients C_1 and C_2 for a given path $\mathcal{P}_i$, current node n, and next node z at a particular thread $\mathcal{T}_i$ and network setting are depicted in Fig. 6. In Fig. 6(a), the inverse link entanglement gradient is $\theta_{E_{L_l}(n,z)}^z = 0.5$, while in Fig. 6(b), it has the value of $\theta_{E_{L_l}(n,z)}^z = 0.2$.

Achievable Entanglement Fidelity in the Protocol. Assuming an ideal recovery operation $\mathcal{R}$ with an optimal quantum error correction $\mathcal{C}$[12–33,41–45,48] in the proposed routing mechanism, the F entanglement fidelity is evaluated as

$$F = \left\langle \widetilde{\Psi} | \mathcal{R}(\rho_f) | \widetilde{\Psi} \right\rangle, \tag{56}$$

where $\widetilde{\Psi}$ is a shared Bell pair between the final stations, while ρ_f is the input density matrix of $\mathcal{R}$.

For an L_l-level entangled link $E_{L_l}(A, B)$ with hop-distance $d(A, B)_{L_l} = 2^{l-1}$ between final stations A and B, and per-node error probability P_{err} (that includes the effective logical error probability Q and other residual errors ε_{res} in the nodes) in the $d(A, B)_{L_l} + 1$ total stations, after some calculations the entanglement fidelity (56) can be rewritten as[41]
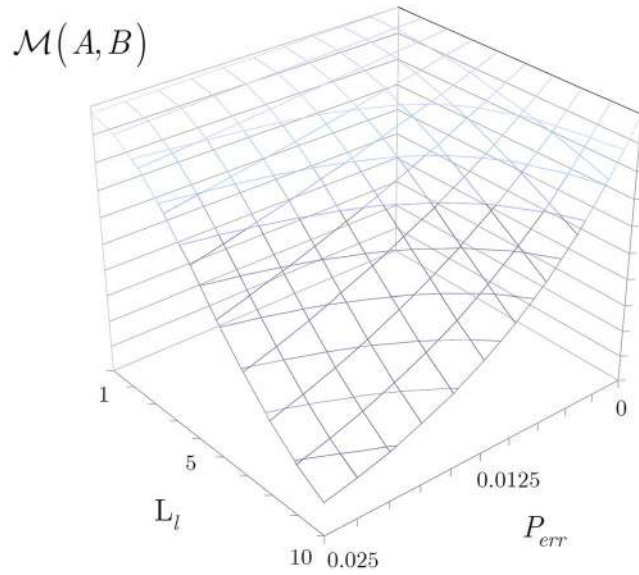
Figure 7. The F entanglement fidelity as obtainable from the correlation measurement $\mathcal{M}(A, B) \approx \sqrt{F}$ between final stations A and B, at per-node error probability $P_{err} = [0, 0.025]$, hop distance $d(A, B)_{L_l} = 2^{l-1}$, and entanglement level $L_l = [1, 10]$.

$$F = (1 - P_{err})^{2\left(d(A,B)_{L_l}+1\right)-2}$$
$$=(1 - (Q + \varepsilon_{res}))^{2d(A,B)_{L_l}}. \tag{57}$$

The performance of the routing is approachable by the correlation measurement $\mathcal{M}(A, B)$ between the final stations A and B, which quantity practically yields the corresponding fidelity information as[41]

$$\mathcal{M}(A, B) \approx \sqrt{F}$$
$$\approx (1 - P_{err})^{d(A,B)_{L_l}+1}$$
$$=(1 - (Q + \varepsilon_{res}))^{2^{l-1}+1}. \tag{58}$$

The results for $\mathcal{M}(A, B)$ in function of per-node error probability P_{err}, and level L_l of the entangled link $E_{L_l}(A, B)$ between the final stations A and B are depicted in Fig. 7.

In the protocol, the F entanglement fidelity of the final Bell pair $\widetilde{\Psi}$ between A and B (see (57)) achieves a theoretical maximum at $d(A, B)_{L_l} - 1$ intermediate quantum repeaters, and at operators $\mathcal{R}$ and $\mathcal{C}$[33,47] Using P_{err}, the $P_{succ}^{tot}(\mathcal{R})$ total success probability of the recovery operation $\mathcal{R}$ for the intermediate nodes is evaluated as

$$P_{succ}^{tot}(\mathcal{R}) = (1 - P_{err})^{2\left(\left(d(A,B)_{L_l}+1\right)-2\right)} = (1 - (Q + \varepsilon_{res}))^{2\left(d(A,B)_{L_l}-1\right)}, \tag{59}$$

while the internal error-correction operation $\mathcal{C}$ has a $P_{succ}^{\widetilde{\Psi}}(\mathcal{C})$ success probability with respect to the final state $\widetilde{\Psi}$ as

$$P_{succ}^{\widetilde{\Psi}}(\mathcal{C}) = (1 - (Q + \varepsilon_{res}))^2. \tag{60}$$

The success probabilities in (59) and (60) yield an estimation[33,47] for the entanglement fidelity F of $\widetilde{\Psi}$ as

$$F \approx P_{succ}^{tot}(\mathcal{R})P_{succ}^{\widetilde{\Psi}}(\mathcal{C}), \tag{61}$$

which therefore practically yields (57).

Security of the Protocol. Based on the F entanglement fidelity (57) of $\widetilde{\Psi}$, the security of the protocol can be characterized[33,47] as follows. At a particular final key K (a shared bitstring between A and B), the proposed protocol guarantees that the maximum information leaked to an eavesdropper E (Eve) is upper bounded[33] as

$$I(E: K) \leq 2^{-c} + 2^{\mathcal{O}(-2s)}, \tag{62}$$

where $I(E: K)$ is the mutual information of Eve, and

$$c = s - \log_2\left(2 + s + \frac{1}{\ln 2}\right),\tag{63}$$

while s is evaluated as

$$s = -\log_2(1 - F),\tag{64}$$

at a particular entanglement fidelity F (57) of $\widetilde{\Psi}$.

The protocol therefore also provides a practical framework to realize quantum key distribution over long distances.

Conclusions

In this work, we defined the entanglement-gradient routing method for quantum repeater networks. The routing scheme is based on the fundamentals of swarm intelligence in order to find the optimal shortest path in entangled quantum networks. We defined the terms of entanglement utility and link and path entanglement gradient, and proposed the routing metrics. The routing metrics are derived from the characteristics of entangled links, entanglement throughput capabilities, and the distribution of the entangled states. The method allows for moderate complexity routing in quantum repeater networks by fusing the relevant characteristics of entanglement distribution and swarm intelligence theory. The scheme can be directly applied in quantum networking, future quantum Internet, and experimental long-distance quantum communications. As a future work, we are planning to prepare a transmission analysis and performance comparisons with other schemes.

References

1. Van Meter, R. *Quantum Networking*. ISBN 1118648927, 9781118648926, John Wiley and Sons Ltd (2014).
2. Imre, S., Gyongyosi, L. *Advanced Quantum Communications - An Engineering Approach*. New Jersey, Wiley-IEEE Press (2012).
3. Van Meter, R., Satoh, T., Ladd, T. D., Munro, W. J. & Nemoto, K. Path Selection for Quantum Repeater Networks. *Networking Science* **3**, 82–95 (2013).
4. Van Meter, R., Ladd, T. D., Munro, W. J. & Nemoto, K. System Design for a Long-Line Quantum Repeater. *IEEE/ACM Transactions on Networking* **17**, 1002–1013 (2009).
5. Lloyd, S. *et al*. Infrastructure for the quantum Internet. *ACM SIGCOMM Computer Communication Review* **34**, 9–20 (2004).
6. Hanzo, L. *et al. Proceedings of the IEEE* **100**, 1853–1888 (2012).
7. Lloyd, S., Mohseni, M. & Rebentrost, P. Quantum principal component analysis. *Nature Physics* **10**, 631 (2014).
8. Lloyd, S. Capacity of the noisy quantum channel. *Physical Rev. A* **55**, 1613–1622 (1997).
9. Gyongyosi, L. Quantum Imaging of High-Dimensional Hilbert Spaces with Radon Transform. *International Journal of Circuit Theory and Applications.*, https://doi.org/10.1002/cta.2332 (2017).
10. Yuan, Z. *et al*. Experimental demonstration of a BDCZ quantum repeater node. *Nature* **454**, 1098–1101 (2008).
11. Di Caro, G., Ducatelle, F. & Gambardella, L. M. AdHocNet: An Adaptive Nature-Inspired Algorithm for Routing in Mobile Ad-Hoc Networks. *European Transactions on Telecommunications* **16**, 443–455 (2005).
12. Chou, C. *et al*. Functional quantum nodes for entanglement distribution over scalable quantum networks. *Science* **316**(5829), 1316–1320 (2007).
13. Kimble, H. J. The quantum Internet. *Nature* **453**, 1023–1030 (2008).
14. Gyongyosi, L. The Correlation Conversion Property of Quantum Channels. *Quantum Information Processing* **13**, 467–473 (2014).
15. Kok, P. *et al*. Linear optical quantum computing with photonic qubits. *Rev. Mod. Phys.* **79**, 135–174 (2007).
16. Gisin, N. & Thew, R. Quantum Communication. *Nature Photon.* **1**, 165–171 (2007).
17. Enk, S. J., Cirac, J. I. & Zoller, P. Photonic channels for quantum communication. *Science* **279**, 205–208 (1998).
18. Briegel, H. J., Dur, W., Cirac, J. I. & Zoller, P. Quantum repeaters: the role of imperfect local operations in quantum communication. *Phys. Rev. Lett.* **81**, 5932–5935 (1998).
19. Dur, W., Briegel, H. J., Cirac, J. I. & Zoller, P. Quantum repeaters based on entanglement purification. *Phys. Rev. A* **59**, 169–181 (1999).
20. Duan, L. M., Lukin, M. D., Cirac, J. I. & Zoller, P. Long-distance quantum communication with atomic ensembles and linear optics. *Nature* **414**, 413–418 (2001).
21. Van Loock, P. *et al*. Hybrid quantum repeater using bright coherent light. *Phys. Rev. Lett* **96**, 240501 (2006).
22. Zhao, B., Chen, Z. B., Chen, Y. A., Schmiedmayer, J. & Pan, J. W. Robust creation of entanglement between remote memory qubits. *Phys. Rev. Lett.* **98**, 240502 (2007).
23. Goebel, A. M. *et al*. Multistage Entanglement Swapping. *Phys. Rev. Lett.* **101**, 080403 (2008).
24. Simon, C. *et al*. Quantum Repeaters with Photon Pair Sources and Multimode Memories. *Phys. Rev. Lett.* **98**, 190503 (2007).
25. Tittel, W. *et al*. Photon-echo quantum memory in solid state systems. *Laser Photon. Rev.* **4**, 244–267 (2009).
26. Sangouard, N., Dubessy, R. & Simon, C. Quantum repeaters based on single trapped ions. *Phys. Rev. A* **79**, 042340 (2009).
27. Dur, W. & Briegel, H. J. Entanglement purification and quantum error correction. *Rep. Prog. Phys.* **70**, 1381–1424 (2007).
28. Munro, W. J., Harrison, K. A., Stephens, A. M., Devitt, S. J. & Nemoto, K. From quantum multiplexing to high-performance quantum networking. *Nature Photon.* **4**, 792–796 (2010).
29. Sangouard, N., Simon, C., de Riedmatten, H. & Gisin, N. Quantum repeaters based on atomic ensembles and linear optics. *Rev. Mod. Phys.* **83**, 33–80 (2011).
30. Collins, O. A., Jenkins, S. D., Kuzmich, A. & Kennedy, T. A. Multiplexed Memory-Insensitive Quantum Repeaters. *Phys. Rev. Lett.* **98**, 060502 (2007).
31. Ralph, T. C., Hayes, A. J. F. & Gilchrist, A. Loss-Tolerant Optical Qubits. *Phys. Rev. Lett.* **95**, 100501 (2005).
32. Kwiat, P. G. Hyper-entangled states. *J. Mod. Opt.* **44**, 2173–2184 (1997).
33. Lo, H. K. & Chau, H. F. *Science* **283**, 2050 (1999).
34. Shor, P. W. Scheme for reducing decoherence in quantum computer memory. *Phys. Rev. A* **52**, R2493–R2496 (1995).
35. Bonabeau, E., Dorigo, M. & Theraulaz, G. *Swarm Intelligence: From Natural to Artificial Systems*. ISBN 0-19-513159-2, Oxford University Press (1999).
36. Meuleau, N. & Dorigo, M. Ant Colony Optimization and Stochastic Gradient Descent. *Artificial Life* **8**, 103–121 (2002).
37. Roth, M. & Wicker, S. Termite Ad-hoc Networking with Stigmergy. *The Second Mediterranean Workshop on Ad-Hoc Networks*. 2937–2941, https://doi.org/10.1109/GLOCOM.2003.1258772 (2003).
38. Roth, M. & Wicker, S. Performance Evaluation of Pheromone Update in Swarm Intelligent MANETs. *Mobile and Wireless Communication Networks* 335–346, https://doi.org/10.1007/0-387-23150-1_29 (2005).

39. Simone, G., Gadia, D., Farup, I. & Rizzi, A. Ant Colony for Locality Foraging in Image Enhancement. *Multiobjective Swarm Intelligence* (Editors: Dehuri, S., Jagadev, A. K. & Panda, M). Springer, 123-142 (2015).
40. Roth, M. & Wicker, S. Asymptotic Pheromone Behavior in Swarm Intelligent MANETs: An Analytical Analysis of Routing Behavior. *Mobile and Wireless Communications Networks*. 335–346, https://doi.org/10.1007/0-387-23150-1_29 (2004).
41. Xiao, Y. F. & Gong, Q. Optical microcavity: from fundamental physics to functional photonics devices. *Science Bulletin* **61**, 185–186 (2016).
42. Zhang, W. *et al.* Quantum Secure Direct Communication with Quantum Memory. *Phys. Rev. Lett.* **118**, 220501 (2017).
43. Biamonte, J. *et al.* Quantum Machine Learning. *Nature* **549**, 195–202 (2017).
44. Lloyd, S. Mohseni, M. & Rebentrost, P. Quantum algorithms for supervised and unsupervised machine learning. *arXiv:1307.0411* (2013).
45. Dijkstra, E. W. A note on two problems in connexion with graphs. *Numerische Mathematik* **1**(1), 269–271 (1959).
46. Roth, M. *Termite: A Swarm Intelligent Routing Algorithm for Mobile Wireless Ad-Hoc Networks*. PhD Thesis, Cornell University (2005).
47. Jiang, L. *et al.* Quantum repeater with encoding. *Phys. Rev. A* **79**(3), 032325 (2009).
48. Sheng, Y. B. & Zhou, L. Distributed secure quantum machine learning. *Science Bulletin* **62**, 1025–2019 (2017).

Acknowledgements

Author Contributions

L.GY. designed the protocol and wrote the manuscript. L.GY. and S.I. analyzed the results. All authors reviewed the manuscript.

Additional Information

Supplementary information accompanies this paper at https://doi.org/10.1038/s41598-017-14394-w.

Competing Interests: The authors declare that they have no competing interests.

Publisher's note: Springer Nature remains neutral with regard to jurisdictional claims in published maps and institutional affiliations.